DOI: 10.1111/jeu.12903

ORIGINAL ARTICLE

Journal of Eukaryotic Microbiology ISOP Published by the International Society of Protistologists

Successful invasion of *Trypanosoma cruzi* trypomastigotes is dependent on host cell actin cytoskeleton

Bruno Souza Bonifácio[1] | **Alexis Bonfim-Melo**[1,2] | **Renato Arruda Mortara**[1] | **Éden Ramalho Ferreira**[1]

[1]Departamento de Microbiologia, Imunologia e Parasitologia, Universidade Federal de São Paulo, São Paulo, Brazil

[2]The University of Queensland Diamantina Institute, Faculty of Medicine, The University of Queensland, Woolloongabba, QLD, Australia

Correspondence
Renato Arruda Mortara and Éden Ramalho Ferreira, Departamento de Microbiologia, Imunologia e Parasitologia, Escola Paulista de Medicina, Universidade Federal de São Paulo. Rua Botucatu, 862, Vila Clementino, São Paulo 04023-062, SP, Brazil.
Emails: ramortara@unifesp.br (RAM) and edendearaujo@gmail.com (ÉRF)

Present address
Éden Ramalho Ferreira, Department of Biology, York Biomedical Research Institute, The University of York, Wentworth Way, Heslington, York, UK.

Funding information
The authors thank FAPESP for the grants 2016/15000-4, 2016/16918-5, 2017/24701-9, 2016/17770-1, and CAPES. Renato Mortara is the recipient of a CNPq fellowship (302068/2016-3).

Abstract

Cellular invasion by *Trypanosoma cruzi* metacyclic trypomastigotes (MTs) or tissue culture trypomastigotes (TCTs) is a complex process involving host–parasite cellular and molecular interactions. Particularly, the involvement of host cell actin cytoskeleton during trypomastigote invasion is poorly investigated, and still, the results are controversial. In the present work, we compare side by side both trypomastigote forms and employ state-of-the-art live-cell imaging showing for the first time the dynamic mobilization of host cell actin cytoskeleton to MT and TCT invasion sites. Moreover, cytochalasin D, latrunculin B, and jasplakinolide-pretreated cells inhibited MT and TCT invasion. Furthermore, our results demonstrated that TCT invasion decreased in RhoA, Rac1, and Cdc-42 GTPase-depleted cells, whereas MT invasion decreased only in Cdc42-and RhoA-depleted cells. Interestingly, depletion of the three studied GTPases induced a scattered lysosomal distribution throughout the cytosol. These observations indicate that GTPase depletion is sufficient to impair parasite invasion despite the importance of lysosome spread in trypomastigote invasion. Together, our results demonstrate that the host cell actin cytoskeleton plays a direct role during TCT and MT invasion.

KEYWORDS
actin cytoskeleton, cell invasion, metacyclic trypomastigote, Rho GTPases, tissue culture trypomastigote, *Trypanosoma cruzi*

THE protozoan parasite *Trypanosoma cruzi* causes Chagas' disease, which affects 6–7 million people worldwide, mostly in Latin America. *T. cruzi* has a complex life cycle that includes invertebrate as well as vertebrate hosts. Previous studies have reported that each *T. cruzi* form interacts differently with the host, activating different signaling cascades for mammalian cell invasion (Bonfim-Melo et al., 2018; Ferreira et al., 2012; Maeda et al., 2012). Metacyclic trypomastigotes (MTs) and tissue culture trypomastigotes (TCTs) interact with diverse molecules to invade the host cells. Among the surface molecules, the gp85/transialidase superfamily members gp82 and Tc85 interact with MT and TCT, respectively (Alves & Colli, 2007). In addition, trypomastigote interaction with the host cell membrane triggers host Ca^{2+} signaling, leading to lysosomal scattering and consequent parasite internalization and parasitophorous

vacuole formation (Fernandes et al., 2011; Tardieux et al., 1992). A lysosomal-independent pathway for TCT invasion has also been proposed, where the parasites rely on a PI3K-dependent mechanism in which PIP3 accumulates in parasite interaction sites, culminating in membrane invagination and consequent parasite internalization (Burleigh, 2005; Cortez et al., 2016).

The actin cytoskeleton has essential functions in eukaryotic cells and is responsible for promoting internal vesicle traffic, stress fibers, signaling, cell division, and endocytosis (Spiering & Hodgson, 2011). During actin filament polymerization by the Arp2/3 complex, some nucleation-promoting factors are activated by a GTPase, primarily from the Rho family. Rho GTPases act in different ways in the cell, mainly regulating gene expression, membrane transport, cell adhesion, stress fiber formation, filopodia, and lamellipodia. Three Rho GTPases, Cdc42, RhoA, and Rac1, are mostly involved in actin cytoskeleton modulation (Nobes & Hall, 1999).

Few studies have evaluated actin cytoskeleton participation in trypomastigote host cell invasion, and the available findings remain controversial. Studies on TCTs incubated with cytochalasin D- or jasplakinolide-treated mammalian cells reported a reduced trypomastigote invasion. In addition, the removal of these drugs from the medium restored trypomastigote infectivity (Rosestolato et al., 2002). In contrast, Ferreira et al. (2006) demonstrated that actin participation during MT invasion is strain-dependent. In addition, Mortara (1991) demonstrated that compared with extracellular amastigote invasion, trypomastigote invasion is less affected by host cell treatment with cytochalasin D. Furthermore, studies on macrophages have indicated that actin filaments participate in the trypomastigote invasion associated with PI3K signaling, which consequently activates a phagocytosis-like mechanism (De Souza, 2002). Although TCTs and MTs engage different pathways for internalization, the results presented here demonstrate that both forms use the host cell actin cytoskeleton during the invasion.

EXPERIMENTAL PROCEDURES

Cell cultures

HeLa (human uterine cervical epithelial cells) and Vero cells (monkey kidney epithelial cells green) (Institute Adolfo Lutz) were, respectively, used for assays and to maintain the *T. cruzi* cycle in vitro, as described previously (Procópio et al., 1998). The cells were grown in RPMI 1640, containing 10% fetal calf serum (FCS), and maintained at 37°C in a humid atmosphere with 5% CO_2. HEK293T cells (human renal embryonic cells) were cultured in complete Dulbecco's modified Eagle's medium (DMEM; Sigma–Aldrich). The TCTs were obtained from the supernatant of infected Vero cells cultured in RPMI medium, containing 2.5% FCS, at 37°C in a humid atmosphere with 5% CO_2. The epimastigotes were grown in liver infusion tryptose medium (pH 7.2), supplemented with 10% FCS, at 27°C; the MTs were obtained after incubating the epimastigotes in Grace medium at 27°C and were purified on a diethylaminoethyl cellulose column, as previously described (Yoshida, 1983). *T. cruzi* from CL strain (*T. cruzi* VI (Zingales et al., 2009)) were used in all experiments.

Lentiviral transduction and establishment of depleted HeLa cell lineages

HeLa cell lines, stably expressing the interfering RNA sequences for Cdc42, RhoA, and Rac1, used in this project had previously been established in our laboratory (Bonfim-Melo, et al., 2018). The sequences obtained commercially (Sigma–Aldrich) are presented below, and the lentiviruses were produced according to the protocol described (Bonfim-Melo et al., 2015). A suspension of 5×10^6 HEK293T cells was seeded in 10 cm dishes with complete DMEM. After 24 h, the cells were transfected by calcium phosphate precipitation with a 15 μg shRNAi vector (pLKO.1), 10 μg viral protein (pdR8.9), and 5 μg VSV-G envelope (pCI.VSVG) per dish. After 6 h, the cells were incubated with 15% glycerol in phosphate-buffered saline (PBS) for 2 min, washed twice with PBS, and incubated with a complete medium. After 24 and 48 h of transfection, the culture supernatant was filtered through a 0.45 μm pore membrane and stored at −80°C. For lentiviral transduction, 5×10^4 HeLa cells were seeded in a 6-well plate and 1 ml lentivirus supernatant was added to cells with 8 μg/ml polybrene® (Sigma–Aldrich) after 24 h. The supernatant was completely replaced 24 h post-transduction and shRNAi-expressing cells were selected using increasing puromycin concentrations (from 0.2 to 10 μg/ml) in the following 2 weeks. Protein depletion was evaluated using standard western blotting protocols. The primary antibodies used were anti-Rac1 mouse mAb (clone 23A8; Millipore), anti-RhoA rabbit pAb (R9404, Sigma–Aldrich). anti-Cdc42 mouse pAb (EPR15620; Abcam), and anti-β-actin mouse mAb (3700; Cell Signaling), while the secondary antibodies used were goat anti-rabbit IgG-peroxidase (A6154; Sigma–Aldrich) and anti-mouse IgG-peroxidase (A4416; Sigma–Aldrich). Chemiluminescence reaction was performed using the ECL Prime western blotting detection kit (Amersham Biosciences) and assessed on an Alliance 2.7 photodocumenter (UVitec). pLKO1 plasmids

containing the shRNAi oligos, purchased from Sigma–Aldrich, were as follows: Cdc42/NM_001791 (TRCN0000299931; CCGGCCTGATATCCTACACAACAAACTCGAGTTTGTTGTGTAGGATATCAGGTTTTTG), Rac1/NM_006908 (TRCN0000318375; CCGGCCCTACTGTCTTTGACAATTACTCGAGTAATTGTCAAAGACAGTAGGGTTTTTG), RhoA/NM_001664 (TRCN0000047711; CCGGTGGAAAGACATGCTTGCTCATCTCGAGATGAGCAAGCATGTCTTTCCATTTTTG), and Scramble/Scr (SHC001; CCGGCAACAAGATGAAGAGCACCAACTCGAGTTGGTGCTCTTCATCTTGTTGTTTTTG). The lentivirus-packing plasmids pdR8.9 and pCI.VSVG have been previously used by our group (Bonfim-Melo et al., 2015, 2018).

Invasion assays

For assays with depleted HeLa cells, 1.5×10^5 cells/well were plated in a 24-well plate and incubated at 37°C. After 24 h, MTs or TCTs were added (MOI 25) and the plates were incubated for 2 h at 37°C and 5% CO_2. The coverslips were then stained with Giemsa. Intracellular parasites were counted in 500 cells/coverslip, in quadruplicate.

Giemsa staining

The coverslips used for Giemsa staining were washed six times with PBS to remove noninternalized parasites, fixed with Bouin (Sigma–Aldrich) for 5 min, washed five times with PBS, stained with Giemsa (1:4 in tap water) for 1 h, and sequentially dehydrated in acetone, followed by a graded series of acetone:xylol (9:1, 7:3, and 3:7) and finally xylol. This technique allows the optic distinction between intracellular parasites, which are surrounded by a halo. The coverslips were then mounted on slides with Entellan (Merck) and analyzed using optical microscopy, as described previously (Ferreira et al., 2017).

For assays with drugs that impair actin cytoskeleton dynamics, 1.5×10^5 HeLa cells were plated per well in a 24-well plate. After 24 h, the cells were treated with 20 µM cytochalasin D (Kustermans et al., 2005; Legrand-Poels et al., 2007; Lin et al., 2018), 4 µM latrunculin B (Ferreira et al., 2006), and 0.1 µM jasplakinolide (Lin et al., 2018; Rosestolato et al., 2002), (Sigma–Aldrich). Cell viability tests showed that the treatment did not cause a significant change in cell viability (revealed by morphology recovery after drug removal). After 1 h of treatment, cells were washed thrice with PBS to remove the drugs and incubated with MTs and TCTs (MOI 25) for 2 h at 37°C and 5% CO_2. Giemsa staining protocol was followed. Intracellular parasites were counted in 500 cells/coverslip in triplicate.

Immunofluorescence

Cells on the coverslips were gently washed with PBS, fixed with 3% paraformaldehyde and 0.2% glutaraldehyde (0.1% or 0.2% of glutaraldehyde combined with 3%–4% of paraformaldehyde has been shown to improve the fixation since it fixes faster and more completely, consequently generating more preserved cell structures Richter et al., 2018; Tanaka et al., 2010) for 15 min at room temperature (22–25°C), and stained with 4,6-diamidino-2-phenylindole (DAPI, #1306, Sigma–Aldrich), phalloidin-TRITC (Sigma–Aldrich) and the respective specific PGN-Saponin-diluted antibodies for each experiment (Bonfim-Melo et al., 2015), for 1 h. For lysosome localization mouse mAb anti-lamp2 antibody (H4B4, Thermo) was diluted 1:100 and subsequently reacted with Alexa Fluor-488 anti-mouse IgG (Invitrogen) 1:200 as a secondary antibody. The coverslips were mounted on slides with 1 mM glycerol-*p*-phenylenediamine (Sigma–Aldrich) buffer before evaluation using epifluorescence (BX51; Olympus) or confocal (TCS SP5 II Tandem Scanner; Leica) microscopes. Lysosomal spread index was performed by measuring the lysosome signal distributed throughout the cytoplasm subtracted from the perinuclear region on ImageJ using the Freehand selection tool followed by a Measurement tool. GraphPad Prism was used for statistical analysis.

Actin recruitment assays

For the time-lapse assay, HeLa cells were plated in Hi-Q4 (ibidi) plates for 24 h and transfected with 2 µg LifeAct-GFP and 6 µl FuGene HD according to the manufacturer's instructions. The next day, the medium was replaced and 48 or 72 h post-transfection, the cells were incubated with Lysotracker (Invitrogen) (for labeling and tracking acidic organelles in live cells) for 1 h. Then, MTs or TCTs were added (MOI 25) and interactions were evaluated using time-lapse confocal microscopy. The cells were incubated at 37°C with 5% CO_2 in a humid atmosphere. Five focal planes were acquired (0.7-µm thickness and 2-µm z-step), with 3–4 min intervals, using 63X and 1.40 N.A. objective. At

least four fields were evaluated in two independent experiments. Confocal images were processed and rendered with IMARIS 7.0.0 (Bitplane) and evaluation of actin and lysosome dynamics during parasite interaction was performed with ImageJ. Twenty-two events were analyzed in two independent experiments.

For actin recruitment assays with fixed cells, 10^5 HeLa cells per well were plated on coverslips in 24-well plates. After 24 h, MTs and TCTs were added to the wells (MOI 25) for 1 h, after which the coverslips were subjected to the immunofluorescence protocol. Invading parasites were counted and actin recruitment in each interaction was evaluated (100 interactions per coverslip). Representative images were acquired with confocal microscopy and edited using the IMARIS 7.0.0 (Bitplane) software.

Statistical analysis

Results are presented as mean ± SD. Each point represents a replicate from independent duplicate, triplicate, or quadruplicate experiments. Analyses were performed using ANOVA with Tukey's multiple comparison test using the GraphPad Prism 7.0® software.

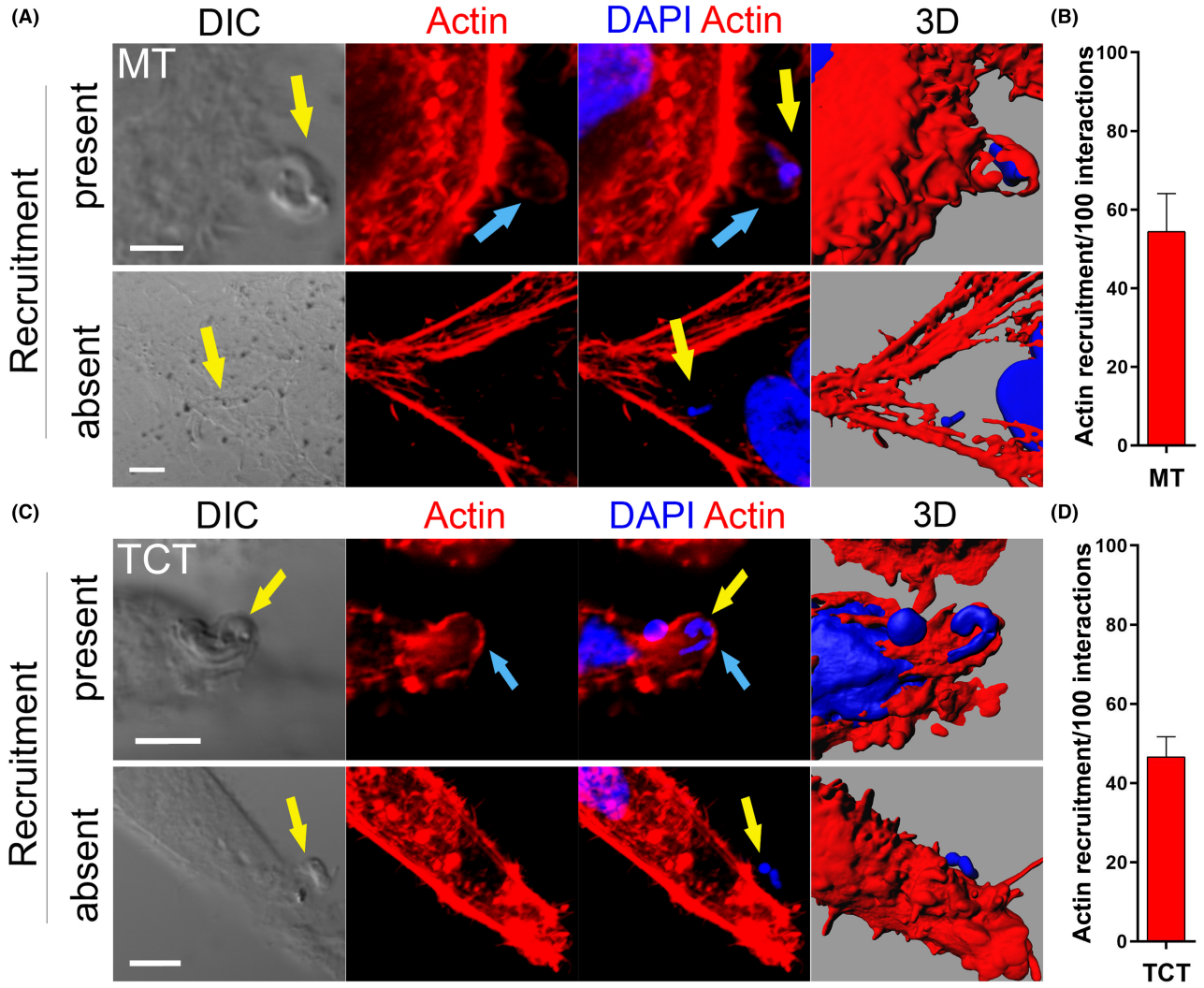

FIGURE 1 Trypomastigotes selectively recruit host cell actin cytoskeleton to membrane adhesion site. HeLa cells were incubated with (A) metacyclic trypomastigotes (MTs) or (C) tissue culture trypomastigotes (TCTs) fixed with paraformaldehyde and stained with 4,6-diamidino-2-phenylindole (DAPI; nucleic acid marker) and phalloidin-TRITC (filamentous actin marker). Yellow and blue arrows show the adhered MTs and actin recruitment by the parasite, respectively. 3D: three-dimensional surface renderization showing recruitment or not of actin to the parasite invasion site. Bar: 5 µm. (B, D) F-actin recruitment quantification in at least 100 parasites per replicate (three independent experiments, in triplicate)

RESULTS AND DISCUSSION

Actin participates in MT and TCT invasion

To elucidate the role of the actin cytoskeleton during trypomastigote invasion, we first incubated HeLa cells with TCTs and MTs for 1 h and then fixed the cells to observe the F-actin using fluorescent microscopy. Interestingly, approximately half of the interactions displayed actin recruitment to the invasion sites of both forms (Figure 1A–D). However, confocal live-cell imaging experiments, using HeLa cells transfected with Lifeact-GFP, revealed that both MT and TCT were internalized only after actin recruitment (Figure 2A,B). Furthermore, Figure 2C,D indicate adherent

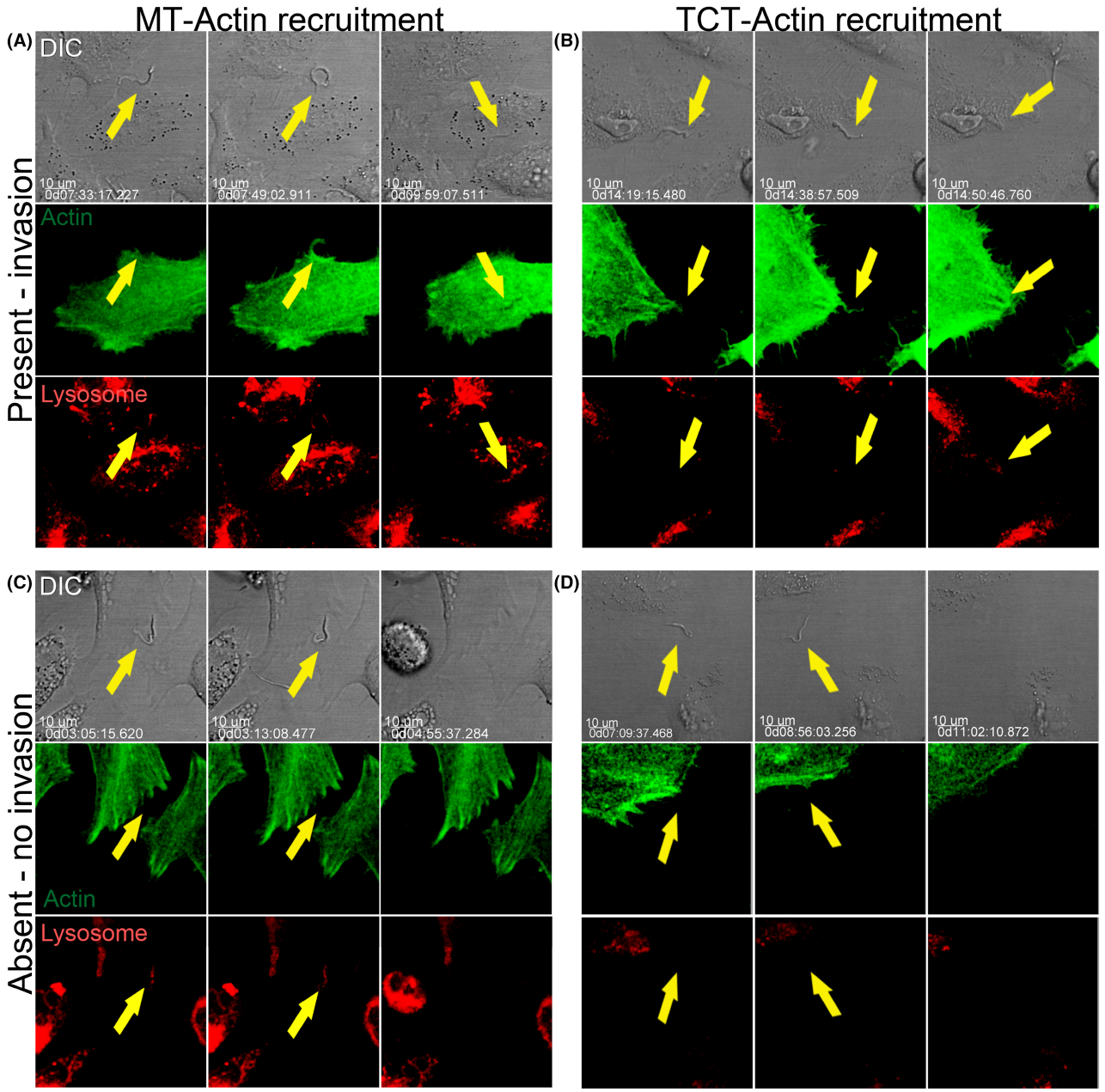

FIGURE 2 F-actin recruitment is required for trypomastigote internalization. HeLa cells were transfected with the Plasmid Lifeact-GFP (green) and incubated with Lysotracker (red) for visualization of actin and lysosome dynamics, using confocal live-cell imaging, during interaction with MTs and TCTs. (A and B) Interaction of MT and TCT with the host cell actin cytoskeleton results in successful parasite internalization. All observed internalizations were followed by actin recruitment. (C and D) No actin recruitment to trypomastigote invasion site results in parasite detachment from the host cell membrane. Particularly for MTs, lysosomes are recruited to the adherent parasites regardless of actin recruitment without internalization (C). Arrowheads indicate the parasites. Bar = 10 μm. Images were edited and processed using Imaris (Bitplane) and ImageJ (NIH open source)

parasites without actin recruitments, which are consequently not internalized. The interactions shown in Figure 2 can be found on Videos S1–S4. Video S1 shows actin recruitment and MT internalization, and Video S2 shows the opposite, with no actin recruitment and consequently no internalization. Videos S3 and S4 show the same pattern in TCTs (internalization with actin recruitment and no internalization with no actin recruitment, respectively).

Thus, parasites can adhere to the cells, as observed by lysosome recruitment (MT); however, internalization is completed only after F-actin recruitment.

Additionally, with live-cell imaging we were able to elucidate temporal aspects of actin and lysosome dynamics during trypomastigote invasion. For MTs, lysosome accumulation occurs before actin recruitment and the contrary occurs for TCTs. Both actin and lysosomes remain recruited until TCT and MT internalization. Table 1 shows the average time of actin and lysosomes dynamic during trypomastigote invasion. The fact that MTs recruit lysosomes before F-actin suggests the higher dependency of lysosomal recruitment from MTs than TCTs for invasion. In addition, during live-cell experiments, we observed parasites that are not internalized but still temporarily accumulate actin. Therefore, we could not find any temporal pattern in these interactions. Comparable results were obtained during the invasion of *T. cruzi* extracellular amastigotes. In previous works from our group, we demonstrated that the depletion of the ERM proteins or the here studied GTPases (Bonfim-Melo et al., 2018; Ferreira et al., 2017) leads to a significantly delayed internalization but the actin dynamics and recruitment to invasion site was still preserved displaying same features as WT cells. We conclude that invasion of trypomastigotes is dependent on an efficient actin cytoskeleton signaling cascade that may not be triggered in all interactions.

Thus, it can be inferred that actin plays a role in trypomastigote invasion. Several studies have previously given clues on the host cell membrane and actin recruitment, using fluorescence microscopy, but little has been concluded. Ferreira et al. (2006) demonstrated that actin recruitment by trypomastigotes is apparently strain-dependent since only the G strain presented actin recruitment to its invasion site (compared with the CL strain). Precisely, they probably observed the selective recruitment of actin, which was believed to be strain-dependent at that time. Instead, selective actin recruitment to the parasite invasion site occurred in the same strain in the same experiment, as presented here. In this study, we revealed the selective nature of actin recruitment for successful parasite internalization, using live-cell imaging coupled with F-actin probes. Furthermore, Mortara (1991) had previously described the selective fashion of actin recruitment to parasite attachment sites. In addition, scanning electron microscopy results of previous studies have revealed membrane projections toward interacting trypomastigotes, which may be indirectly associated with actin-driven mobilization (Nogueira & Cohn, 1976; Schenkman & Mortara, 1992).

To corroborate the involvement of actin filaments in trypomastigote invasion, we determined whether the use of cytochalasin D, latrunculin B, and jasplakinolide, drugs, which act on the actin cytoskeleton, impairs trypomastigote invasion (Lin et al., 2018; Osuna et al., 1993; Rosestolato et al., 2002). HeLa cells were pre-treated with the drugs, which reduced both MT and TCT invasion (Figure 3A,B). Although previous studies have reported the effect of some of these drugs on MT or TCT invasion (Ferreira et al., 2006; Mortara, 1991; Osuna et al., 1993; Rosestolato et al., 2002), we present, for the first time, the effect of all four drugs on both MT and TCT using the same system. In addition, we have previously demonstrated that cytochalasin D almost abolishes extracellular amastigote invasion, which is highly dependent on actin cytoskeleton rearrangement (Bonfim-Melo et al., 2018; Ferreira et al., 2012; Mortara, 1991; Procópio et al., 1998). Since we observed a significant reduction in MT and TCT invasion, but not as pronounced as extracellular amastigote invasion reduction, we may infer that the actin cytoskeleton participates during trypomastigote invasion but to a lesser extent. These results also corroborate the notion that different routes are important for MT and TCT internalization (Burleigh, 2005; Cortez et al., 2016; Fernandes et al., 2011).

TABLE 1 Average time of actin and lysosomes dynamic during trypomastigote invasion

	Time (min)				
	Attachment	**Actin recruitment**	**Lysosome accumulation**	**Invasion**	**Actin dispersal**
MT	0	4	4	140	144
TCT	0	4	24	46	50

Note: Twenty-two events were analyzed in two independent experiments. For MTs, we observed that lysosomes recruitment takes place prior to actin recruitment. For TCTs, first we observe actin recruitment and then lysosomal accumulation. Both actin and lysosomes remain recruited until TCT and MT internalization. Noteworthy, the internalization time disposed here is useful to show the relation between invasion, actin, and lysosomes dynamics during the invasion. The total interaction time (attachment to invasion) observed here may not necessarily correspond to all different *Trypanosoma cruzi* strains and even for the different experimental conditions performed with CL strain (used in this study).

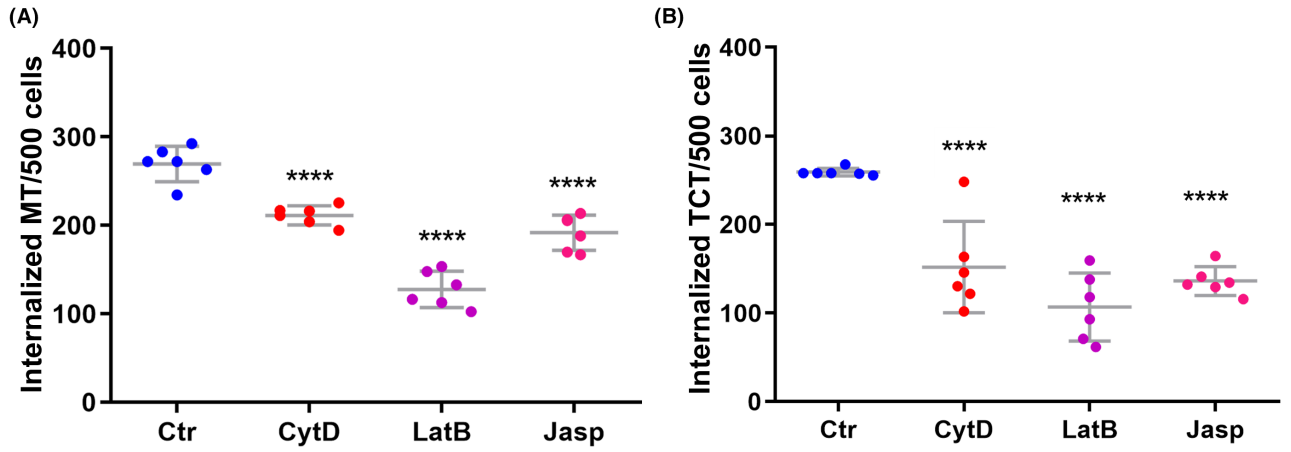

FIGURE 3 Impairment of the host cell actin cytoskeleton inhibits metacyclic trypomastigote (MT) and tissue culture trypomastigote (TCT) invasion. (A, B) HeLa cells were pretreated with cytochalasin D, latruculin B, and jasplakinoline for 1 h. Then, the cells were washed and incubated with the parasites (MOI 25). Pretreatment with all drugs inhibited MT and TCT invasion compared to that in the nontreated group (Ctr). The data correspond to the mean of two independent experiments performed in triplicate (three coverslips per group in each experiment). Intracellular parasites were counted in 500 cells/coverslip. ± SD ****$p < 0.0001$ and ***$p < 0.001$. Statistical analysis was performed with ANOVA using Tukey's multiple comparison method

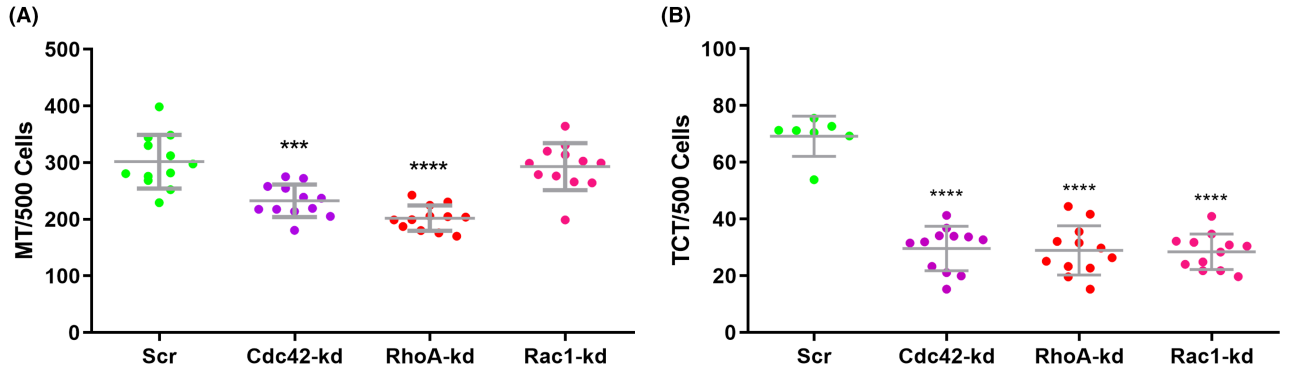

FIGURE 4 Rho GTPase depletion significantly inhibits trypomastigote invasion. (A and B) Cdc42, RhoA, or Rac1-depleted HeLa cells were incubated with metacyclic trypomastigotes (MTs) or tissue culture trypomastigotes (TCTs) for 2 h (MOI 25). The number of internalized parasites was counted using epifluorescence microscopy. (A) Cdc42 and RhoA, but not Rac1, depletion significantly inhibited MT invasion. (B) Cdc42, RhoA, and Rac1 depletion significantly inhibited TCT invasion. Data correspond to the mean of three experiments performed in quadruplicate (four coverslips per group in each experiment), and the intracellular parasites were counted in 500 cells/coverslip. ± SD ****$p < 0.0001$. Statistical analysis was performed using ANOVA with Tukey's multiple comparison method

Participation of Rho GTPases during trypomastigote invasion

Previous studies have reported that Rho GTPases are key regulators of actin dynamics and subverted by diverse intracellular parasites (Spiering & Hodgson, 2011). Additionally, the participation of Rho GTPases during cell invasion by extracellular *T. cruzi* amastigotes has been reported (Bonfim-Melo, et al., 2018). Since we initially observed that actin participates in cell invasion by trypomastigotes, we investigated whether Cdc42, RhoA, and Rac1 GTPases participate in TCT and MT invasion. Hence, we established Cdc42, RhoA, or Rac1-depleted HeLa cells using lentiviral transduction and demonstrated that cell invasion by MTs was reduced by Cdc42 and RhoA, but not Rac1, depletion (Figure 4A). Depletion of all three Rho GTPases inhibited TCT invasion (Figure 4B). Figure S1 shows HeLa cell lineages with shRNAi-knocked down Cdc-42, RhoA, or Rac1, as assessed with western blotting. In contrast, Rac1 plays a pivotal role in extracellular amastigote invasion, followed by a less prominent role of Cdc-42 and a nonsignificant part of RhoA (Bonfim-Melo et al., 2018). From these results, it can be concluded that regulating Rac1-driven lamellipodia formation (Spiering & Hodgson, 2011) is central to extracellular amastigote invasion, and actin dynamic disturbances driven by overall Rho GTPase depletion might impact its participation during trypomastigote invasion.

Finally, owing to the importance of host cell lysosomal distribution in trypomastigote invasion (Cortez et al., 2016; Fernandes et al., 2011; Woolsey & Burleigh, 2004), we evaluated the lysosomal distribution in Cdc-42-, RhoA-, and Rac1-depleted cells, using confocal microscopy. Interestingly, our results demonstrated that depletion of the three

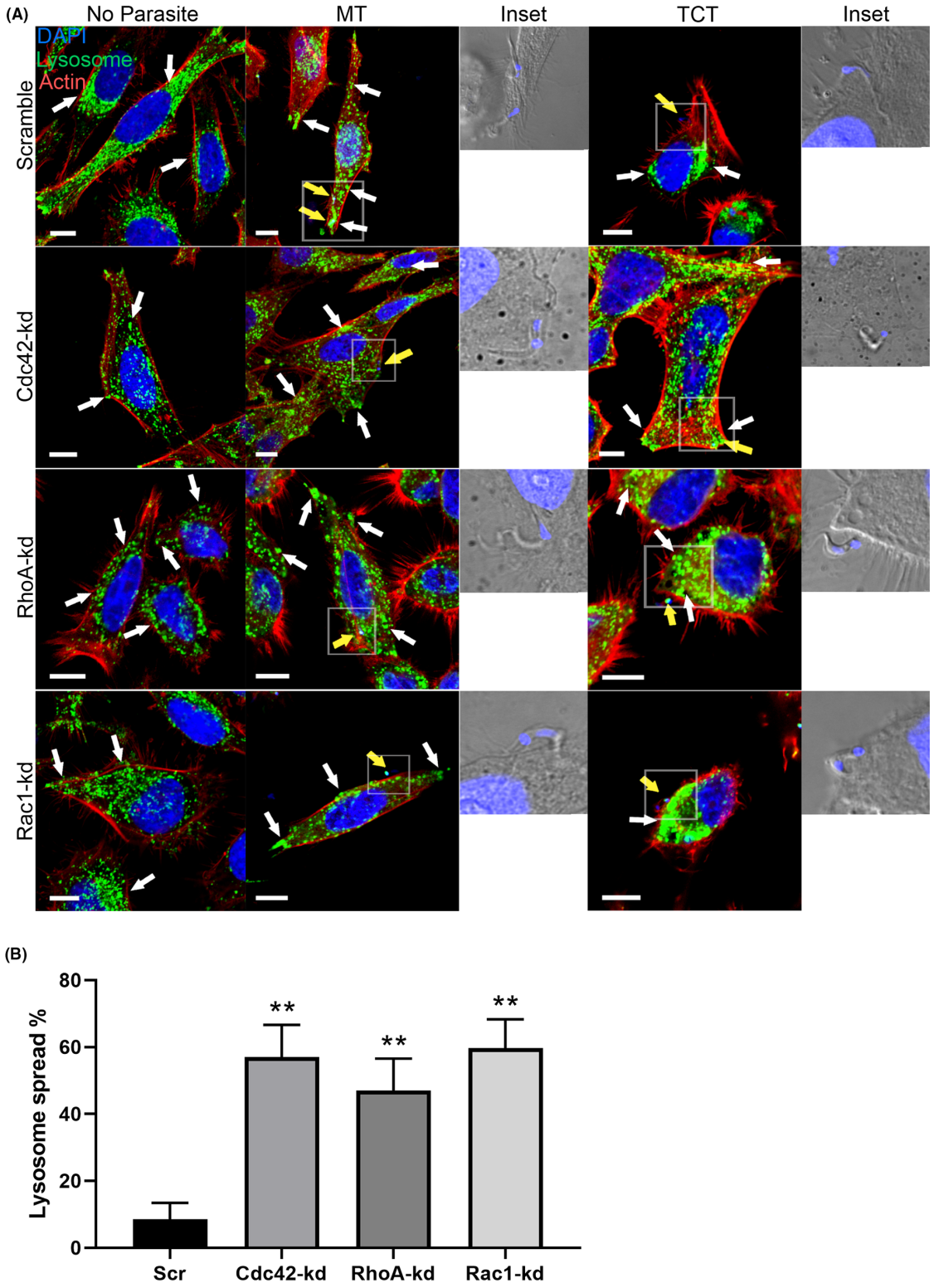

FIGURE 5 Rho GTPases, Cdc-42, RhoA, and Rac1 depletion increase lysosomal spread in HeLa cells. (A) HeLa cells stably depleted for Cdc-42, RhoA, or Rac1 were incubated, or not, with metacyclic or tissue culture trypomastigotes (arrows) and immunofluorescence using anti-lamp2 (specific lysosomal marker, green), 4,6-diamidino-2-phenylindole (DAPI, nuclei specific, blue) and kinetoplast and phalloidin-TRITC, red (F-actin specific). Lysosomal distribution (white arrows) was evaluated using confocal microscopy. Two experiments were performed in triplicate. Yellow arrows indicate parasites interacting with the host cell, better viewed in the inset items. Bar: 10 μm. (B) Lysosomes are significantly more spread in cells depleted to Cdc-42, RhoA, and Rac1 when compared to the control group (Scramble). Measurements of anti-lamp2 intensity show lysosomal spread index throughout the cytoplasm. The analyses were performed on ImageJ using the Measurement tool subtracting perinuclear lysosome fluorescent signal from lysosome signal throughout the cytoplasm. ± SD $^{**}p < 0.001$ and $^{***}p < 0.001$. Statistical analysis was performed with ANOVA using Tukey's multiple comparison method

studied Rho GTPases resulted in significantly increased lysosomal dispersion throughout the cytoplasm compared to that in the control group (scramble transduced group), which presents marked perinuclear lysosomal distribution (Figure 5A,B). In addition, incubating Rho GTPase-depleted cells with TCTs and MTs did not affect the already dispersed distribution of lysosomes in these cells. Intriguingly, trypomastigote, particularly MT, invasion is known to cause lysosomal spread (Cortez et al., 2016; Fernandes et al., 2011). Andrews (1993) suggested that lysosomal migration occurs only after cortical F-actin depolymerization. This is in accordance with the dispersed lysosomal distribution observed in Rho GTPase-depleted cells since Rho GTPase depletion might downregulate normal actin dynamics. Noteworthy, since we observed that GTPase depletion have less effect on inhibition of MT invasion (especially for Rac1 depletion in which we did not observe any effect) we may infer that the higher dependency of lysosome spread by MTs compared to TCT (Burleigh, 2005; Cortez et al., 2016) might have counterbalanced the effect of GTPases depletion during MT invasion. Thus, we concluded that though the lysosomal spread is important, it does not superimpose the importance of functional actin (caused by Rho GTPase depletion in this study) for successful trypomastigote internalization.

Taken together the results presented here shed light on previous works and bring strong evidence of the participation of actin cytoskeleton during trypomastigote invasion. We highlight here the novelty of our results, in particular the study of TCT and MT side by side and the live-cell imaging experiments showing vividly the accumulation of actin to trypomastigotes invasion site. Further experiments should be conducted to explore the relationship between the established mechanisms for trypomastigote invasion and the participation of the host-cell actin cytoskeleton.

ACKNOWLEDGMENTS

The authors thank Prof. Nobuko Yoshida for providing *T. cruzi* CL strain and Wiley (https://wileyeditingservices.com/en/) for English Editing Services.

CONFLICT OF INTERESTS

Authors declare no competing or financial interests.

AUTHOR CONTRIBUTIONS

Study conceptualization: R.A.M., E.R.F., and A.B.M. Study designing: E.R.F and A.B.M. Experimentation: B.S.B., E.R.F., and A.B.M. Result interpretation: E.R.F., A.B.M., R.A.M., and B.S.B. Manuscript writing: E.R.F. and B.S.B.

ORCID

Bruno Souza Bonifácio https://orcid.org/0000-0002-8501-4254
Alexis Bonfim-Melo https://orcid.org/0000-0002-7812-7701
Renato Arruda Mortara https://orcid.org/0000-0002-2311-8349
Éden Ramalho Ferreira https://orcid.org/0000-0001-6534-0426

REFERENCES

Alves, M.J. & Colli, W. (2007) *Trypanosoma cruzi*: adhesion to the host cell and intracellular survival. *IUBMB Life*, 59(4–5), 274–279. https://doi.org/10.1080/15216540701200084

Andrews, N.W. (1993) Living dangerously: how *Trypanosoma cruzi* uses lysosomes to get inside host cells, and then escapes into the cytoplasm. *Biological Research*, 26(1–2), 65–67.

Bonfim-Melo, A., Ferreira, E.R., Florentino, P.T.V. & Mortara, R.A. (2018) Amastigote synapse: the tricks of *Trypanosoma cruzi* extracellular amastigotes. *Frontiers in Microbiology*, 9, 1341. https://doi.org/10.3389/fmicb.2018.01341

Bonfim-Melo, A., Ferreira, E.R. & Mortara, R.A. (2018) Rac1/WAVE2 and Cdc42/N-WASP participation in actin-dependent host cell invasion by extracellular amastigotes of *Trypanosoma cruzi*. *Frontiers in Microbiology*, 9, 360. https://doi.org/10.3389/fmicb.2018.00360

Bonfim-Melo, A., Zanetti, B.F., Ferreira, E.R., Vandoninck, S., Han, S.W., Van Lint, J. et al. (2015) *Trypanosoma cruzi* extracellular amastigotes trigger the protein kinase D1-cortactin-actin pathway during cell invasion. *Cellular Microbiology*, 17(12), 1797–1810. https://doi.org/10.1111/cmi.12472

Burleigh, B.A. (2005) Host cell signaling and *Trypanosoma cruzi* invasion: do all roads lead to lysosomes? *Science's STKE*, 2005(293), pe36. https://doi.org/10.1126/stke.2932005pe36

Cortez, C., Real, F. & Yoshida, N. (2016) Lysosome biogenesis/scattering increases host cell susceptibility to invasion by *Trypanosoma cruzi* metacyclic forms and resistance to tissue culture trypomastigotes. *Cellular Microbiology*, 18(5), 748–760. https://doi.org/10.1111/cmi.12548

De Souza, W. (2002) Basic cell biology of *Trypanosoma cruzi*. *Current Pharmaceutical Design*, 8(4), 269–285.

Fernandes, M.C., Cortez, M., Flannery, A.R., Tam, C., Mortara, R.A. & Andrews, N.W. (2011) *Trypanosoma cruzi* subverts the sphingomyelinase-mediated plasma membrane repair pathway for cell invasion. *The Journal of Experimental Medicine*, 208(5), 909–921. https://doi.org/10.1084/jem.20102518

Ferreira, D., Cortez, M., Atayde, V.D. & Yoshida, N. (2006) Actin cytoskeleton-dependent and -independent host cell invasion by *Trypanosoma cruzi* is mediated by distinct parasite surface molecules. *Infection and Immunity*, 74(10), 5522–5528. https://doi.org/10.1128/IAI.00518-06

Ferreira, E.R., Bonfim-Melo, A., Mortara, R.A. & Bahia, D. (2012) *Trypanosoma cruzi* extracellular amastigotes and host cell signaling: more pieces to the puzzle. *Frontiers in Immunology*, 3, 363. https://doi.org/10.3389/fimmu.2012.00363

Ferreira, E.R., Bonfim-Melo, A., Cordero, E.M. & Mortara, R.A. (2017) ERM proteins play distinct roles in cell invasion by extracellular amastigotes of *Trypanosoma cruzi*. *Frontiers in Microbiology*, 8, 2230. https://doi.org/10.3389/fmicb.2017.02230

Kustermans, G., El Benna, J., Piette, J. & Legrand-Poels, S. (2005) Perturbation of actin dynamics induces NF-kappaB activation in myelomonocytic cells through an NADPH oxidase-dependent pathway. *The Biochemical Journal*, 387(Pt 2), 531–540. https://doi.org/10.1042/BJ20041318

Legrand-Poels, S., Kustermans, G., Bex, F., Kremmer, E., Kufer, T.A. & Piette, J. (2007) Modulation of Nod2-dependent NF-kappaB signaling by the actin cytoskeleton. *Journal of Cell Science*, 120(Pt 7), 1299–1310. https://doi.org/10.1242/jcs.03424

Lin, H., Roh, J., Woo, J.H., Kim, S.J. & Nam, J.H. (2018) TMEM16F/ANO6, a Ca(2+)-activated anion channel, is negatively regulated by the actin cytoskeleton and intracellular MgATP. *Biochemical and Biophysical Research Communications*, 503(4), 2348–2354. https://doi.org/10.1016/j.bbrc.2018.06.160

Maeda, F.Y., Cortez, C. & Yoshida, N. (2012) Cell signaling during *Trypanosoma cruzi* invasion. *Frontiers in Immunology*, 3, 361. https://doi.org/10.3389/fimmu.2012.00361

Mortara, R.A. (1991) *Trypanosoma cruzi*: amastigotes and trypomastigotes interact with different structures on the surface of HeLa cells. *Experimental Parasitology*, 73(1), 1–14.

Nobes, C.D. & Hall, A. (1999) Rho GTPases control polarity, protrusion, and adhesion during cell movement. *Journal of Cell Biology*, 144(6), 1235–1244.

Nogueira, N. & Cohn, Z. (1976) *Trypanosoma cruzi*: mechanism of entry and intracellular fate in mammalian cells. *Journal of Experimental Medicine*, 143(6), 1402–1420. https://doi.org/10.1084/jem.143.6.1402

Osuna, A., Rodriguez-Cabezas, N., Boy, M., Castanys, S. & Gamarro, F. (1993) The invasion mechanism of the metacyclic forms of *Trypanosoma cruzi* in nonphagocytic host cells. *Biological Research*, 26(1–2), 19–26.

Procópio, D.O., da Silva, S., Cunningham, C.C. & Mortara, R.A. (1998) *Trypanosoma cruzi*: effect of protein kinase inhibitors and cytoskeletal protein organization and expression on host cell invasion by amastigotes and metacyclic trypomastigotes. *Experimental Parasitology*, 90(1), 1–13. https://doi.org/10.1006/expr.1998.4314

Richter, K.N., Revelo, N.H., Seitz, K.J., Helm, M.S., Sarkar, D., Saleeb, R.S. et al. (2018) Glyoxal as an alternative fixative to formaldehyde in immunostaining and super-resolution microscopy. *EMBO Journal*, 37(1), 139–159. https://doi.org/10.15252/embj.201695709

Rosestolato, C.T., Dutra Jda, M., De Souza, W. & de Carvalho, T.M. (2002) Participation of host cell actin filaments during interaction of trypomastigote forms of *Trypanosoma cruzi* with host cells. *Cell Structure and Function*, 27(2), 91–98.

Schenkman, S. & Mortara, R. A. (1992) HeLa cells extend and internalize pseudopodia during active invasion by Trypanosoma cruzi trypomastigotes. *Journal of Cell Science*, 101(Pt 4), 895–905. https://doi.org/10.1242/jcs.101.4.895

Spiering, D. & Hodgson, L. (2011) Dynamics of the Rho-family small GTPases in actin regulation and motility. *Cell Adhesion and Migration*, 5(2), 170–180.

Tanaka, K.A.K., Suzuki, K.G.N., Shirai, Y.M., Shibutani, S.T., Miyahara, M.S.H., Tsuboi, H. et al. (2010) Membrane molecules mobile even after chemical fixation. *Nature Methods*, 7(11), 865–866. https://doi.org/10.1038/nmeth.f.314

Tardieux, I., Webster, P., Ravesloot, J., Boron, W., Lunn, J.A., Heuser, J.E. et al. (1992) Lysosome recruitment and fusion are early events required for *trypanosome* invasion of mammalian cells. *Cell*, 71(7), 1117–1130.

Woolsey, A.M. & Burleigh, B.A. (2004) Host cell actin polymerization is required for cellular retention of *Trypanosoma cruzi* and early association with endosomal/lysosomal compartments. *Cellular Microbiology*, 6(9), 829–838. https://doi.org/10.1111/j.1462-5822.2004.00405.x

Yoshida, N. (1983) Surface antigens of metacyclic trypomastigotes of *Trypanosoma cruzi*. *Infection and Immunity*, 40(2), 836–839.

Zingales, B., Andrade, S.G., Briones, M., Campbell, D.A., Chiari, E., Fernandes, O. et al. (2009) A new consensus for *Trypanosoma cruzi* intraspecific nomenclature: second revision meeting recommends TcI to TcVI. *Memorias do Instituto Oswaldo Cruz*, 104(7), 1051–1054.

SUPPORTING INFORMATION

Additional supporting information may be found in the online version of the article at the publisher's website.

How to cite this article: Bonifácio, B.S., Bonfim-Melo, A., Mortara, R.A. & Ferreira, É.R. (2022) Successful invasion of *Trypanosoma cruzi* trypomastigotes is dependent on host cell actin cytoskeleton. *Journal of Eukaryotic Microbiology*, 69, e12903. https://doi.org/10.1111/jeu.12903